

See discussions, stats, and author profiles for this publication at: <https://www.researchgate.net/publication/241243293>

Interferometric figure metrology: enabling in-house traceability

Article in Proceedings of SPIE - The International Society for Optical Engineering · June 2001

CITATIONS

2

READS

51

4 authors:



Chris Evans

University of North Carolina at Charlotte

157 PUBLICATIONS 6,489 CITATIONS

SEE PROFILE



Angela Davies

University of North Carolina at Charlotte

61 PUBLICATIONS 530 CITATIONS

SEE PROFILE



Tony L. Schmitz

University of North Carolina at Charlotte

297 PUBLICATIONS 5,531 CITATIONS

SEE PROFILE



Robert E. Parks

The University of Arizona

300 PUBLICATIONS 1,576 CITATIONS

SEE PROFILE

Some of the authors of this publication are also working on these related projects:



Optical standards [View project](#)



In Situ Metrology for Metal Additive Manufacturing [View project](#)

PROCEEDINGS OF SPIE

[SPIDigitalLibrary.org/conference-proceedings-of-spie](https://spiedigitallibrary.org/conference-proceedings-of-spie)

Interferometric figure metrology: enabling in-house traceability

Christopher J. Evans
Angela D. Davies
Tony L. Schmitz
Robert E. Parks

SPIE.

Interferometric figure metrology; enabling in-house traceability

Chris J. Evans*, Angela Davies* Tony Schmitz*, and Robert E. Parks#

* National Institute of Standards and Technology, Manufacturing Metrology Division, Stop 8220,
Gaithersburg, MD 20899-8220

Optical Perspectives Group, Tucson, AZ

ABSTRACT

The basic goal of the Advanced Optics Metrology program in NIST's Manufacturing Engineering Laboratory is to help industry ensure that their measurement results of optical figure and wavefront are traceable. This paper underscores the importance of traceability and reviews the facilities and projects dedicated to achieving that objective.

Keywords: Traceability, uncertainty, interferometer, wavefront, figure

1. INTRODUCTION

Commercial transactions in optical components and systems, like any other commodity, are based more or less explicitly on compliance with a set of specifications which may relate to imaging performance, wavefront, or individual component dimensions or material properties. In the absence of any specific contractual language defining acceptance test procedures, it must be assumed that traceable measurement results are used as the basis for a claim of conformance (or otherwise) with the specification. However, the steps needed to make a traceable measurement of optical figure or wavefront are typically not rigorously adhered to in the optical fabrication community in general; Section 2 of this paper will give an overview of basic traceability concepts and indicate their application to optical figure metrology.

As will be seen in Section 2, a critical step to performing a traceable measurement of optical figure is the development of an uncertainty statement. This became even more significant with the international ratification of ISO 14253 Part 1¹ which provides the basic decision rules for conformance testing; again, in the absence of contractual language to the contrary, the terms of ISO 14253 Part 1 may apply by default. Paraphrasing, this standard requires that, in deciding if a part meets specification, vendors must subtract the expanded uncertainty of their measurement from the tolerance; buyers, by contrast, add the expanded uncertainty of the measurement made at in-coming inspection. One consequence can easily be understood from a highly simplified example. Suppose company A is building an optical system with a spherical mirror which, functionally, needs to have surface figure errors no greater than 150 nm peak-to-valley (PV). The interferometer used for incoming inspection has an uncorrected figure error of the reference surface of 20 nm which, when combined with other sources of uncertainty (e.g., instrument noise, alignment, etc.) gives an uncertainty of 50 nm. Company A, therefore, decides to be "safe" and contracts with vendor company B to supply the mirror with a figure error of 100 nm PV, knowing that the part must measure worse than 150 nm before they can reject it. If B's final inspection is made on an interferometer with an uncertainty of 40 nm, then the part must measure at better than 60 nm PV before it may be shipped with assurance that it will be accepted.

Good metrology, and hence traceable measurements based on appropriate uncertainty statements, are the basis for fair trade. In addition, uncertainty analyses are a key tool to improving measurements and consequently increasing the fraction of the tolerance available for manufacturing. Performing such analyses in accordance with the requirements of the ISO Guide to the Expression of Uncertainty in Measurement (GUM)² is not widely practiced in the optical fabrication community. The Advanced Optics Metrology Program within NIST's Manufacturing Engineering Laboratory aims to help US industry make traceable measurements of optical figure and wavefronts primarily through the development and publication of appropriate measurement methods and their associated uncertainty analyses. The lowest uncertainty in a specific measurement is usually achieved through the use of "self-calibration" techniques (see Section 2). Some users, however, prefer to achieve traceability through a "calibrated" artifact. Section 2 of this paper discusses the key issues associated with traceability as it applies to the measurement of optical figure. Section 3 describes NIST facilities for optical figure metrology, focussing on a new

instrument that is the program “flagship”. Finally, Sections 4-7 give examples of current measurement projects contributing to the overall program goals through both self-calibration and standard/well-known/characterized artifacts.

2. TRACEABLE RESULTS OF OPTICAL FIGURE MEASUREMENTS

The definition of traceability³ is:

“Property of the result of a measurement or the value of a standard whereby it can be related to stated references, usually national or international standards, through an unbroken chain of comparisons all having stated uncertainties.”

Optical figure measurements are length measurements, reporting departures from nominal geometry in meters (or more usually in some sub-division thereof). Thus, the result of the measurement is traceable if there is a complete, explicitly described, and documented series of comparisons, and associated uncertainties, that link the measurement result with a realization of the meter (and its uncertainty). NIST’s Policy on Traceability clearly states⁴ that:

“providing support for a claim of traceability of the result of a measurement ... is the responsibility of the provider of that result...”

and suggests that:

“To support a claim, the provider of a measurement result or value of a standard must document the measurement process or system used to establish the claim and provide a description of the chain of comparisons that were used to establish a connection to a particular stated reference. There are several common elements to all valid statements or claims of traceability:

- a clearly defined particular quantity that has been measured
- a complete description of the measurement system or working standard used to perform the measurement
- a stated measurement result or value, with a documented uncertainty
- a complete specification of the stated reference at the time the measurement system or working standard was compared to it
- an ‘internal measurement assurance’ program for establishing the status of the measurement system or working standard at all times pertinent to the claim of traceability”

The first of these elements, -- the definition of the measurand -- seems obvious, yet may be the cause of differences that exceed the claimed uncertainties in intercomparisons. Consider, for example, the simple case of the length of a gage block. Without appropriate care in defining “length”, the result of an optical measurement may diverge significantly from a measurement made using mechanical contact with the gage surfaces. Similarly, the measured PV flatness of an optical surface depends, among other things on the mounts used, the spatial resolution of the measuring system, and the exact aperture over which the measurement is made.

From the discussion above, it is clear there are two main routes by which any metrologist can logically support a claim of traceability in the result of a measurement of optical figure: the conventional, hierarchical approach to calibration or through “self-calibration”⁵. The critical features of the hierarchical approach are the following:

- an appropriate artifact for which traceability has been established, in the reported quantity, by some external reference (such as a national measurement institution)
- valid stated uncertainties in the results of the comparison of the artifact with the part measured.

Assuming that the part is to be measured on an interferometer, this process requires an accounting for all significant uncertainty sources when mastering the instrument with the artifact and when measuring the part. In addition, uncertainties arising from the drift of the instrument between mastering cycles, the stability of the artifact, and in the measurement result supplied by the external reference must be included.

Several sources of uncertainty may be avoided by the use of well-known “self-calibration” techniques, such as a three-flat test. Here a claim of traceability in the measurement result, without reference to any external authority, may be supported if:

- the unit of length is realized, with a stated uncertainty, in the measurement process, and
- a defensible uncertainty analysis of the measurement process is developed.

The sources of uncertainty arising in the self-calibration process are essentially the same (although perhaps in different combinations) as in the comparison of a part with a calibrated artifact. Thus choosing self-calibration poses little or no greater difficulty in developing the uncertainty statement than the artifact-based procedure. As indicated above, self-calibration typically also provides for a lower uncertainty; consider the two approaches to a traceable flat measurement where either the user performs a three flat test or calibration service (such as a national measurement institution) performs such a test on a reference artifact provided to the user. In either approach, the unit must be realized. Both organizations suffer the same uncertainty sources in the multiple measurements involved in the three-flat test; in the hierarchical approach, additional uncertainties arise from the transfer and from the extra measurements that must be made. Thus, unless the uncertainties in measurements at the user's facility are substantially larger than at the calibration service, self-calibration will provide lower uncertainty, although it will require more measurements to be made at the user's facility.

An important aspect of traceability is the validation of the "stated uncertainties" which may be achieved by a documented and critically reviewed uncertainty analysis, and/or intercomparisons among independent measurement methods. Note that the "stated uncertainties" implicitly or explicitly depend on a model of the measurement and the sources of uncertainty. Intercomparisons between independent measurement methods may identify cases where a significant source of uncertainty has been overlooked (see Section 5 for an example).

For a typical (phase shifting) interferometric measurement of optical figure using a Helium-Neon (HeNe) laser source, the meter is realized with significantly lower uncertainty than other components of the uncertainty analysis. If the HeNe laser produces reasonably intense red light, it is operating at its nominal 633 nm wavelength in vacuum to within a relative uncertainty of 3×10^{-6} or better⁶. The theoretically possible, but highly unlikely, 612 nm and 640 nm radiations can be removed, if desired, with a narrow bandpass filter, which may be calibrated by some external authority. The interferometric tests measure optical path difference (OPD), which is limited in principle by the Nyquist limit to a maximum of 1 fringe per 2 pixels on the detector, and practically to a somewhat lower fringe density. For a 1024 x 1024 array, the Nyquist limit gives a maximum OPD of approximately 160 μm and an uncertainty component due to vacuum wavelength uncertainty of 0.48 picometers. If the interferometric test is performed in air, as the majority are, then the effective wavelength may differ from the vacuum wavelength by about 3 parts in 10^4 . For the Nyquist limited case, this will introduce a bias of 48 nm, which could be substantially reduced by making the well known corrections (see for example ⁷ and the references therein).

Note that for other light sources, the uncertainty associated with the realization of the unit must be considered separately. Note also that the argument above applies only to the measurement of small optical path differences. If a phase measuring interferometer is used in a Saunders configuration, for example, to measure the diameter of a sphere with reference to an etalon, then the realization of the meter can become a significant contribution to the uncertainty analysis.

If the measurement result is an amplitude description (e.g., PV or a histogram of the surface or wavefront departure from nominal), then the unit (length) needs only to be realized along the optical axis (Z) of the test set-up. Frequently, however, optical surface or wavefront specifications include descriptions in terms of Zernike polynomials, Fourier or power spectral distributions (PSD). Here realization of the unit in the X,Y plane is also required, and the uncertainty analysis must also consider the effect, for example, of distortion on the measurement result.

Care needs also to be exercised in the expression of uncertainty in the measurement of optical figure. If the measurement result is an amplitude parameter, then the expanded uncertainty can be evaluated using the procedures developed in the GUM² and expressed in the usual manner (e.g., PV = (A +/- B) nm) together with a clear statement of the coverage factor used⁸. The procedure defined in the GUM has certain acknowledged limitations; the most relevant to the testing of optics are that it does not explicitly allow the use of prior information (see Estler⁹ for further discussion) and can give rise to counterintuitive expressions of measurement results near physical limits. Amplitude expressions of departure from nominal figure (eg flatness) can only be positive, but the range of "reasonable" values as expressed by the expanded uncertainty may include negative values. For example, we measured the end test masses (ETM) for the Laser Interferometric Gravitational-wave Observatory (LIGO) project at NIST; in the central 150 mm aperture, the figure of ETM 3 (Figure 1) was dominated by spherical aberration which was confirmed by shearing the part with respect to the interferometer. Our best estimate of the root mean square (rms) departure of the surface, after removal of astigmatism (0.28 nm rms) was 0.35 nm; we evaluated the expanded uncertainty as 1 nm, and therefore might express the measurement result as rms = (0.35 +/- 1) nm. Since the rms

cannot be negative, a better expression might have asymmetric uncertainties, ie. $+1\text{nm}$ and -0.35 nm and then the measurement result would be expressed as $\text{rms} = 0.35_{-0.35}^{+1}\text{ nm}$. While there is a statistically significant probability that the part is “perfect”, we know this not to be true; the shearing test (prior information) is not explicitly used in the reduction of data that leads to the measurement result, although logic suggests that the data be used to adjust the reported uncertainty.

If the reported result is a table of coefficients of Zernike polynomials or a PSD, the appropriate expressions of uncertainty are clear. For the Zernikes, an evaluated uncertainty (including uncertainty components associated with both the measurement process and the fitting) can be associated with each reported coefficient. Since the coefficients may be either positive or negative, then there is no conceptual problem if the uncertainty has a larger magnitude than the reported coefficient. For the PSD, the uncertainty may be plotted as what is traditionally called an “error bar” at each point in the reported distribution.

In some cases [e.g., NIST’s measurement of prototype optics for Extreme Ultra-violet Lithography (EUVL) and for the mirrors for the (LIGO)], the reported result is a matrix of heights representing the departure of the surface or wavefront from nominal. Here the uncertainty should be expressed as another matrix, giving the uncertainty at every point. Users of the measurement result have suggested that this is cumbersome, although we are unaware of any standardized alternative that makes the expression of the uncertainty simpler. Visualization of the uncertainty matrix is easy when presented as a map, much as the reported figure error often is. An example is shown in Figure 2, which provides a great deal of information, but does not provide a simple quantification of our state of knowledge about the measurement. One useful approach may be to provide an amplitude description of the uncertainty matrix (eg the peak value or rms). This, however, suppresses information about the spatial distribution of uncertainties, for example that they may be higher at the edge of the aperture or have a spatial content arising from stray light in the measurement. Another approach is to consider the uncertainty matrix as a “bounding” surface which itself could be described by Zernikes (eg Figure 2), Fourier series etc. Note that uncertainties in the Zernike coefficients that fit the surface are not the same as a Zernike description of the uncertainties.

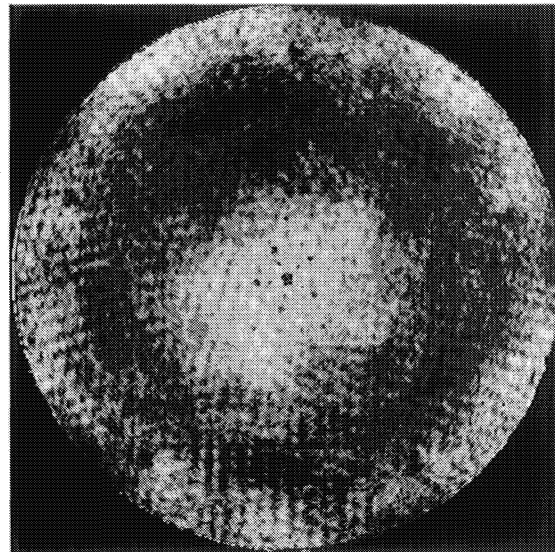


Figure 1. Central 150 mm aperture of LIGO ETM 3. Major contributions are spherical aberration and stray light, observed here with 5 fold symmetry resulting for the 5 position test used¹⁰

3. NIST FACILITIES FOR OPTICAL FIGURE METROLOGY

The Advanced Optics Metrology program in NIST’s Manufacturing Engineering Laboratory uses four different interferometers in two different laboratory environments for measurements of optical figure and wavefront. A general purpose laboratory houses a WYKO 6000 PC¹¹ dual port (150 mm and 45 mm apertures) interferometer operating at 633 nm (Figure) and a prototype Infra-Red Interferometer^R (IR²) (Figure 3) built for NIST by Tropel¹²; a common height for the optical axes of the instruments allows for the use of common tooling. The NIST X-ray optics CALIBration Interferomet^R

(XCALIBIR) is housed in a separate specially designed enclosure that provides excellent environmental control. An ADE PhaseShift¹³ MiniFiz can be used in either area. Both XCALIBIR and the MiniFiz operate at 633 nm source wavelengths.

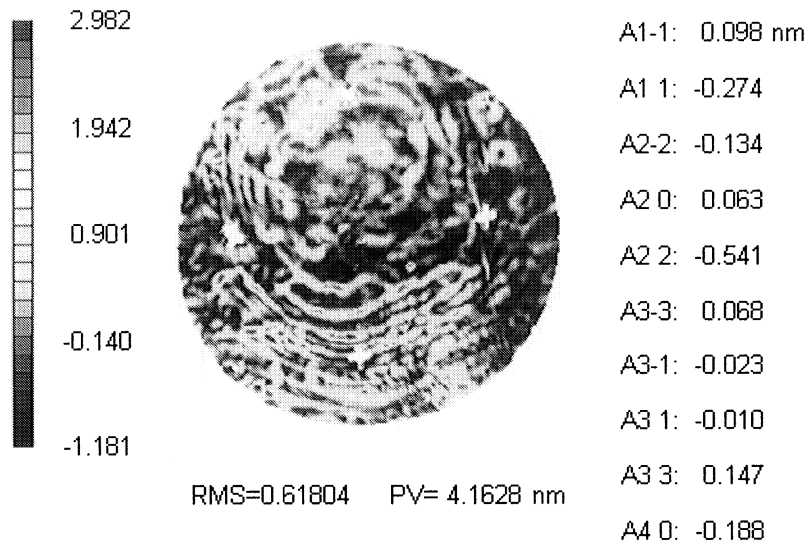


Figure 2: Standard deviation map and Zernikes coefficients for a test of wafer thickness variation in a prototype Haidinger fringe interferometer.

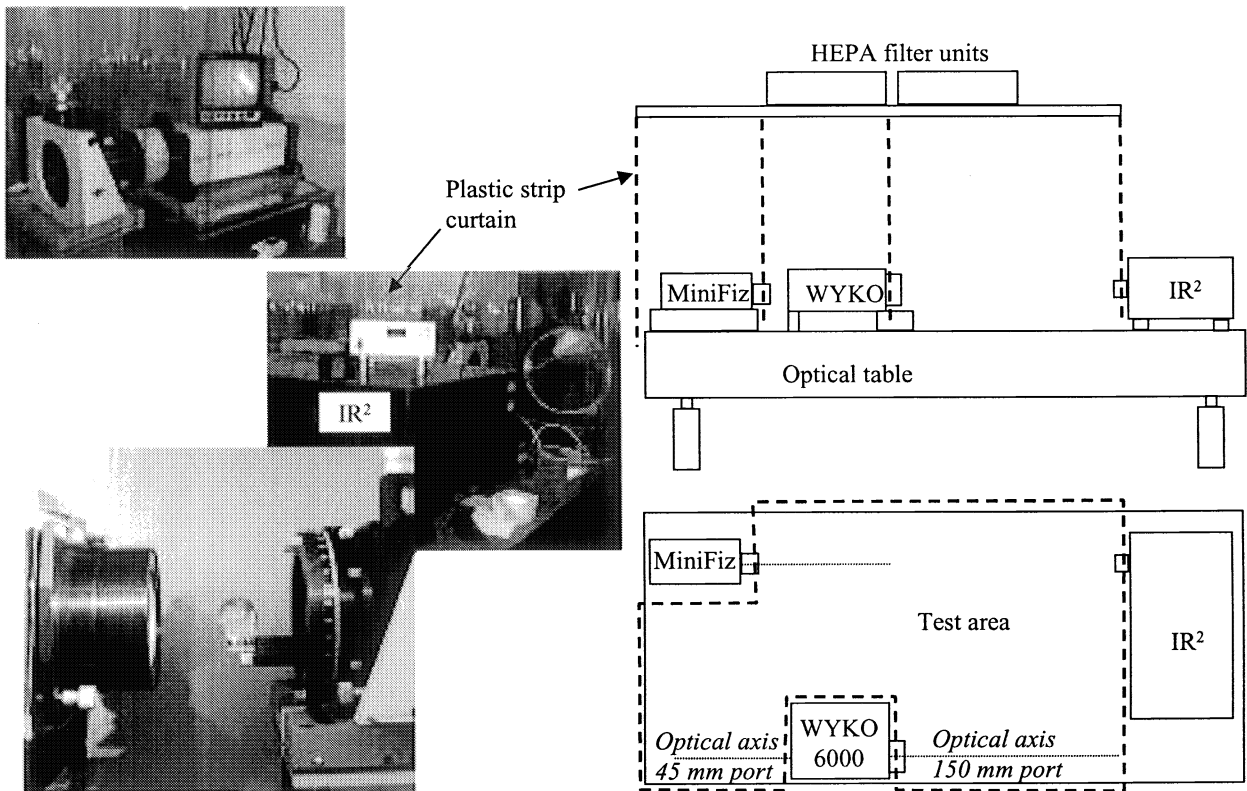


Figure 3: General-purpose test laboratory layout. Optics for each test aperture of each instrument pierce the plastic strip curtain that isolates the test area from the rest of the laboratory.

Environmental effects, most notably temperature, can have a significant, often underestimated effect on optical tests. ISO 1¹⁵ states that the reference temperature for industrial length metrology is 20 °C, a standard that is widely ignored in the optical fabrication and testing communities. At first sight, the standard may seem irrelevant; an optical flat that is “perfect”, for example, at an equilibrium temperature of 20 °C will be equally perfect (over a slightly larger aperture) at an equilibrium temperature of 22 °C. If the flat is mounted in a cell, however, the results may be very different. In a comparison of measurements of a mounted flat at a well-known optics vendor and at NIST we found systematic differences in power and astigmatism. These differences were attributed to changes in loading conditions on the flat as the aluminum cell contracted from the 21 °C at the vendor’s facility to the 20 °C at which the NIST facilities are operated. In measurements of transmitted wavefronts through complex optical systems, changes in temperature produce changes in both dimensions and refractive indices; the concept is well understood, for example, in the military optics community that routinely produces “athermal” designs. The same thermal effects, however, may be observed in the “transmission spheres” provided as accessories for commercially available laser Fizeau interferometers; the uncertainties introduced may be small, but not necessarily negligible when using such instruments to measure radii of curvature¹⁶, for example.

Much more significant uncertainties arise in the presence of temperatures that are varying either temporally and/or spatially. Decades of effort¹⁷ devoted to understanding the effects of temporal variations in more conventional dimensional metrology and ultra-precision manufacturing are captured in ANSI B.89.6.2¹⁸, which predates and, not surprisingly, uses concepts incompatible with the GUM. Considerable effort within ISO TC 213 WG 3 has shown that the central concepts from B.89.6.2 can be transferred to provide guidance on the assessment of uncertainties in the presence of temporally varying temperatures¹⁹. Critical to that assessment is a “drift test” carried out over times longer than the master cycle for the instrument. Common experience with optical testing shows that a drift test which reports amplitude parameters (such as PV and rms) after the removal of rigid body terms (piston and tilt for flats; piston, tilt and power for spherical optics) may show relatively little effect. Much more telling, however, is a drift test where wavefront maps are recorded at regular intervals over an extended period. The average of all maps can be subtracted from the individual maps and typically show significant variations. The results can conveniently be captured in a “map” of the standard deviations of the reported amplitudes at each pixel (Figure 2)

The variations observed in such a drift test arise from mechanical motions of components of the test set-up and changes in indices of glass and air. Tightly enclosed test paths may minimize variations, at the possible price of introducing stationary air stratification. In the general-purpose test laboratory at NIST, we minimize these problems by reducing the thermal load to the test area, while providing controlled air flow through the system. Both interferometers permanently installed in this area (Figure 3) sit on a 5 m x 1.5 m optical table. An independently mounted plenum provides HEPA-filtered air, at an operator adjustable flow rate, to the test area that contains only the interferometer reference optics plus the test optics and mounts. The test area is enclosed by clear plastic strip curtains (overlapped 100 mm strips) which provide easy access for test set-up and adjustment. Long-term temperature variations are within +/- 0.5 °C. We see no evidence of significant temperature stratification but, particularly for long test paths, we do see “turbulence”, ie variations in the local index of the air path. Air flow rates are adjusted such that reasonable averaging controls this contribution to within the limits of the target uncertainty for the measurement.

XCALIBIR is a larger aperture instrument with larger, hence more temperature sensitive mounts, longer air paths, and much tighter target measurement uncertainties. Consequently, temperature must be more carefully controlled. The instrument is in a highly temperature-controlled environment and sits on a pneumatically-isolated 16 metric-ton granite base, which provides a large thermal inertial and vibration isolation from the building (see Figure 5). An active-feedback temperature control systems provide HEPA-filtered air to the measurement enclosure at a rate of approximately two room changes per minute and results in temperature stability much better than 0.05 °C (see Figure 6). Controlling temperature with a large airflow while minimizing turbulence-induced vibration is always a challenging compromise. Software control of the environment allows users to optimize these conditions as needed. To minimize temperature gradients, only two heat sources are in the measurement enclosure - the 1k x 1k CCD detector and the laser head for the displacement measuring interferometers. Temperature stability and uniformity is further improved by eliminating the user heat load during a measurement sequence; various motorized mounts can be remotely controlled and measurement procedures can be scripted and executed from an adjacent room. The temperature gradient over the measurement volume was 0.25 °C after installation (See Figure 7) and has since been reduced to 0.15C with the addition of an independent air-flow flush of the displacement measuring interferometers (DMI) heat source. The temperature gradient is also stable to better than 0.05 °C. Air-flow induced vibration and turbulence

dominate the noise in single measurements, but because the environment is very stable, drift during a longer measurement period is small, so noise can be reduced through averaging.

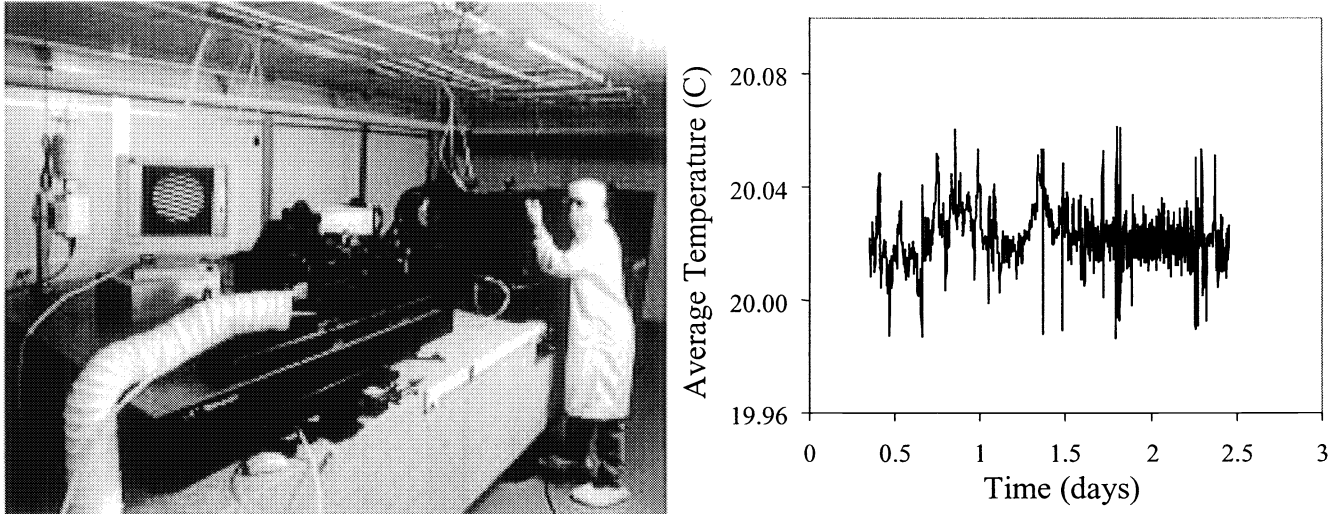


Figure 5 (left): The NIST X-ray optics CALIBration Interferometer (XCALIBIR). Figure 6 (right) Average temperature in XCALIBIR during a two-day drift test. The data are the average of thirty-six sensors in a grid configuration over the measurement volume (see Figure 5). The standard deviation is 0.013 C. The six thermistors monitoring the temperature for the environment feedback control were independent of the thirty-six sensors in the test, consequently the data in the plot are slightly offset from 20.00 C.

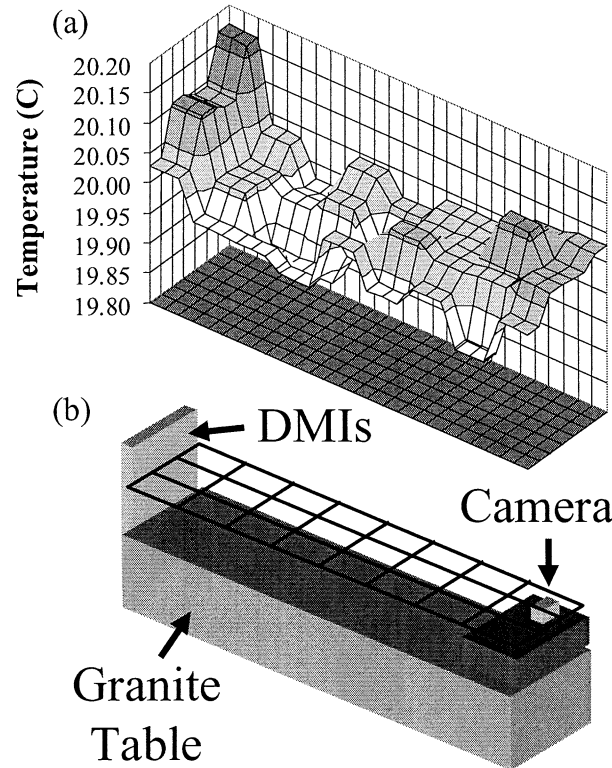


Figure 7: Temperature gradients in XCALIBIR during a two-day drift test. Thirty-six sensors were arranged in a grid over the measurement volume as depicted in part (b). The two heat sources in the room, the camera and the DMIs, cause a modest temperature increase in these areas. Since these data were taken, the heat load from the DMIs has been eliminated, bringing temperatures in this area to values similar to those in the middle of the table.

The instrument itself was designed to be a flexible, general-purpose interferometer that would allow NIST to respond to needs of a diverse customer base. It is a 300 mm aperture instrument with a broad range of optics to allow measurement of: flats; a range of convex or concave spherical parts or wavefronts; and asphere testing with refractive, reflective, or computer-generated holographic nulls. An important design criterion was the ability to test an optic in at least two different configurations, consequently the instrument can be set up as either a Twyman-Green or a Fizeau interferometer. The optics in XCALIBIR are simple and known well enough to allow detailed ray-trace modeling of test setups to remove systematic effects from a non-null test configuration when testing aspheres and/or for evaluating measurement uncertainties in ultra-precision tests. For example, a rotating ground glass optic in the imaging leg, which is commonly used to reduce stray light, is avoided. Also to facilitate ultra precision testing, wavefronts are extremely good, which reduces corrections from non-null conditions and minimizes the residual measurement uncertainty. The instrument operates with 633 nm light from either a frequency-stabilized He-Ne laser or a laser diode. Undesirable stray light can be minimized by either modulating the diode laser source to reduce temporal beam coherence and/or by using extended sources to reduce spatial beam coherence. DMIs can be used to monitor axial motion of the test part, which facilitates radius of curvature measurements and connecting the coordinate system of the test part to the coordinate system of the detector.

The NIST Infrared Interferometer (IR²) was developed to provide thickness and thickness variation information for silicon wafers (up to and including 300 mm diameters) in support of the semiconductor industry. There currently are difficulties in measuring 300 mm wafers and, perhaps more importantly, separating wafer thickness variation from vacuum chuck non-flatness and chuck/wafer interactions. An accurate, independent measurement of wafer geometry is one critical requirement for solving this problem.

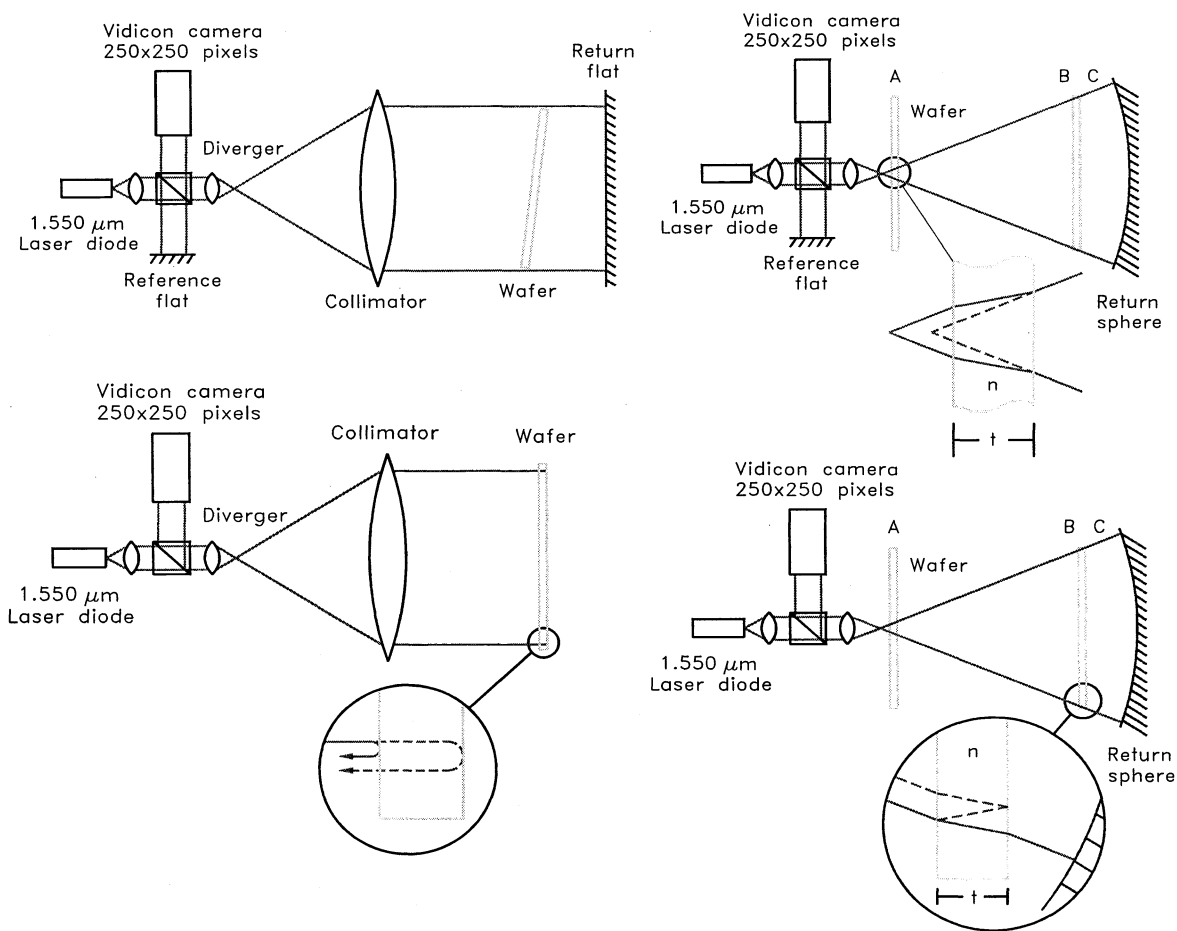


Figure 8: IR² Measurement Configurations (1st row – Twyman-Green, 2nd row – Haidinger fringe, 1st column – collimated wavefront, 2nd column – diverging wavefront)

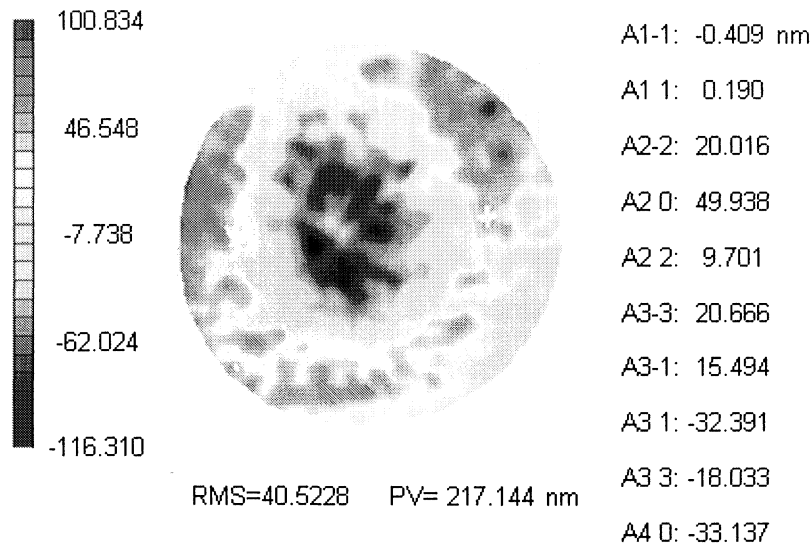


Figure 9: Residual thickness variation measurement for central 150 mm aperture of 200 mm double-side polished wafer (data dropout was caused by fiducials applied to the wafer to identify measurement location)

IR² is fundamentally composed of a tunable wavelength infrared distributed feedback diode laser (nominal beam splitter, a Twyman-Green reference flat, and an f/3 diverger. It may be configured in either of two modes: Twyman-Green or “Haidinger fringe”, where the measurement cavity is defined by the front and back surfaces of the wafer. In either configuration, transmission measurements may be performed using a diverging or collimated wavefront (the reader will recall that silicon is transparent in the infrared and its high index of refraction provides high reflectivities). Four possible measurements setups are shown in Figure 8. In the traditional Twyman-Green configurations, phase shifting is completed by piezo-driven motion of the Twyman-Green reference surface; the Haidinger fringe setups rely on wavelength variation to perform the phase shifting.

An example thickness variation measurement result for the central 150 mm of a 200 mm double-side polished wafer using the collimated wavefront Haidinger fringe configuration is shown in Figure 9. This result displays the residual thickness variation after removing the existing large wedge in the wafer thickness.

4. UNCERTAINTIES IN THE TESTING OF FLATS

Optical testing is an interesting metrology in that often the part to be tested is as good or better than the reference artifact and/or contributions from other systematic effects (such as non-common path errors). Hence, the optical test community has developed many 'self-calibration' test methods (often called 'absolute' test methods), meaning that the test method nominally yields an estimate of the test part in the absence of these errors (for example see^{5,20, 21} and references therein.]. However, in spite of an algorithm that nominally removes all systematic effects, errors still remain (albeit theoretically zero on average), and a determination of the measurement uncertainty is an equally important part of the test. While individual sources of uncertainty in these tests are often discussed in the literature, a demonstration of a complete uncertainty analysis is lacking.

We have recently completed the first self-calibration test on XCALIBIR, carrying out a multi-position 3-flat test¹⁰ on three 300mm optical flats. For this test, the dominant uncertainty sources are from alignment uncertainty, long-term drift of the instrument, vibration, and turbulence. The complete uncertainty analysis for this test is a good example of properly combining these uncertainty sources and arriving at the final statement of measurement uncertainty in accordance with the ISO GUM. This work will be presented at the Optical Manufacturing and Testing IV conference at this year's (2001) SPIE symposium on Optical Science and Technology²².

5. RADIUS

The radius of curvature of spherical surfaces may be determined using the well-known radius bench (i.e., an interferometer with a linear mechanical axis and position transducer). In this method, a phase measuring interferometer is typically employed to identify the null positions at the best fit spherical surface (cat's eye) and center of curvature (confocal) of the test optic. A linear slide provides motion between these positions and one or more displacement measuring interferometers is typically used to record the displacement between the cat's eye and confocal positions and, hence, the radius of curvature. Recent NIST efforts in the analysis and testing of this procedure have focused on identifying the associated uncertainties. Measurements of a polished Zerodur sphere (with an approximate radius of 24.5 mm) have been completed on XCALIBIR using several well-characterized reference spheres ($f/1.1$ to $f/10$) in both the Twyman-Green and Fizeau configurations. Mechanical measurements of the spherical artifact have also been completed using the NIST Moore-48 coordinate measuring machine.

Although good measurement repeatability/reproducibility have been obtained, a large departure among different transmission spheres and the mechanical result has been observed. Using the $f/1.1$ transmission sphere in the Fizeau configuration, for example, an average radius of 24.465719 mm with a standard deviation of 22 nm was recorded over a three-month period (17 measurements with multiple changes in setup); this reproducibility was within the estimated uncertainty based on a model of the measurement using geometric optics and the standard uncertainty sources outlined in the literature. However, the Twyman-Green mode measurements using an $f/4$ diverger, yielded an average radius of 24.466019 mm – a difference of 300 nm. The mechanical measurement provided a radius value of 24.465983 mm with a stated uncertainty of 50 nm, which falls between the $f/1.1$ and $f/4$ results, but not within the predicted uncertainties for the $f/1.1$ result.

An uncertainty analysis of the procedure using standard uncertainty sources outlined in the literature does not account for this level of disagreement. For measurements of the Zerodur sphere performed on XCALIBIR, for example, an expanded uncertainty ($k = 2$) of 52 nm was calculated. Therefore, additional uncertainty contributors are being explored including: 1) focus sensitivity – variation in power with imaging optics focus, 2) aperture stop diffraction, and 3) diffraction effects at focus (i.e., cat's eye) versus confocal. This disagreement between independent measurement methods underscores the importance of cross-checks to identify measurement biases and suggests that, whenever possible, these checks should be included as a critical procedure in the establishment of a defensible uncertainty analysis.

As with the work on flats, more details on the uncertainty analysis and measurement methods will be presented at the Optical Manufacturing and Testing IV conference at this year's SPIE symposium on Optical Science and Technology.

6. BIAS IN RMS

The root mean square (RMS) of the surface or wavefront deformation is a commonly used amplitude description of an optical test result. Not only is the RMS a good statistical representation of the wavefront or surface quality (as opposed to the peak-to-valley value), it is also directly related to the Strehl ratio, which is a measure of imaging performance. Traditionally, the RMS of the measurement result is used as the estimate of the RMS of the surface (or wavefront) departure. However, noise in the measurement, noise that is zero on average, leads to an RMS that is higher on average than the RMS of the true surface departure. For most optical tests, where the noise is much smaller than the surface departure being measured, the bias is small and can be ignored. The bias can be significant, however, in measurements under very noise conditions or in tests of ultra-precision optics. We have illustrated this with a simple 1-dimensional simulation, which is summarized in Figure 10.

A signal (true surface departure) is modeled as a simple sine wave and noise (with different spatial (x -axis) wavelengths) is added to simulate a measurement (see Figure 10(a)). Lower values of 'N' correspond to lower signal to noise ratios ('N' can be thought of as the number of single measurements averaged to improve signal to noise). Many 'measurements' are simulated for each signal-to-noise condition and the average of the 'measured' RMS values is plotted in Figure 10(b). The simulation demonstrates that, for low signal-to-noise, using the simple RMS of the measurement result will be larger than the quantity of interest on average, namely an estimate of the RMS of the *signal*. Hence, particularly in the limit of low signal-to-noise, the RMS of the measurement is not a good estimate of the RMS of the surface departure.

We have developed an analysis algorithm to calculate an unbiased estimate for the RMS of the surface departure and its uncertainty from a dataset²³. By taking multiple measurements and combining the data into sum and difference maps, simple algebraic expressions can be followed to arrive at an unbiased RMS estimate. Most optical tests have a reasonable

signal-to-noise level in which case the more involved calculation is not necessary. The algorithm does, however, yield a straightforward estimate of the RMS uncertainty and therefore is likely worth implementing in many cases. We direct the interested reader to the publication²³ for details.

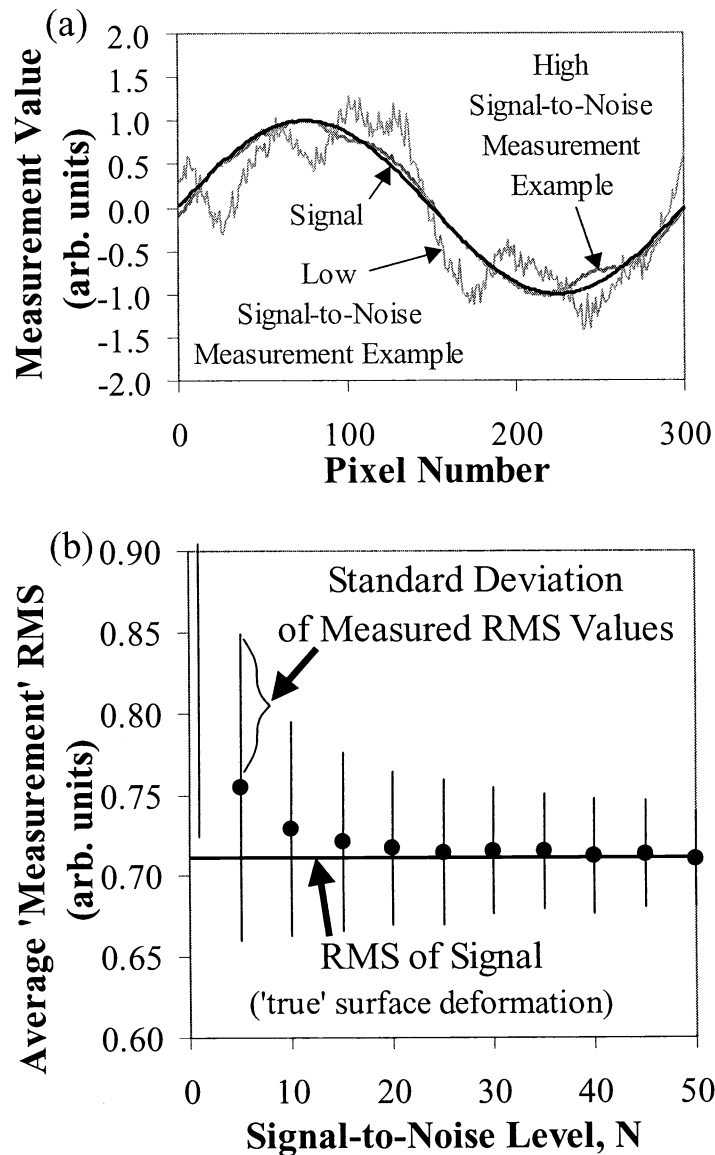


Figure 10: (a) One dimensional simulation of measurements where the 'signal' or surface deformation is modeled as a sine wave and noise of different spatial wavelengths is added. Examples of two different noise conditions are shown. (b) Many 'measurements' such as those shown in part (a) were simulated for each signal-to-noise condition, N . The average RMS of those measurements is plotted versus signal-to-noise level.

7. PHOTOMASKS

The manufacture and metrology of silicon wafers and photomask blanks is expected to improve such that manufacturers of integrated circuits (ICs) can keep pace with Moore's Law, in terms of its representation of demand for ever increasing IC performance. Established metrologies for both components are reaching their limits, provoking a flurry of activity to develop new methods; as indicated above, our focus for wafer metrology is on infrared techniques. For photomasks we are evaluating interferometric techniques in the visible.

Fused silica photomask blanks are typically 152 mm square, 6.25 mm thick, and polished on both sides. If measured in a typical Fizeau interferometer with a long coherence length laser source, reflections from front and rear surface as well as from the reference surface produce a complex interference pattern which cannot be treated by standard phase shifting procedures. The reflections from front and rear surfaces produce a set of static fringes that are variously described as Haidinger or Fabry-Perot fringes. The three beam interference, however, produces apparent wavefront variations that are not directly attributable to dimensions of the part.

As previously discussed [24], the problems posed by rear surface reflections can be mitigated by using a short coherence length source in various interferometric configurations [25,26], mathematically deconvolving the contributions of the two reflections based on precise positioning of the part under test, using grating interferometers [27], or using a diode source and an optical path difference (OPD) that is a multiple of the laser cavity length [28]. None of these approaches can be implemented by users of HeNe-based instruments currently in service. Users of such instruments can frustrate the rear surface reflection using an appropriate index matching fluid or eliminate the reflection by coating the front surface with a highly reflective coating. However, both approaches require subsequent cleaning, and do not address the limited (circular) aperture of most instruments, 100-150 mm versus the needed 215 mm to accommodate the 152 mm square blank. At NIST we are developing two parallel approaches: using the Ritchey-Common configuration in a commercially available interferometer with a long coherence length source, and using a short coherence source on XCALIBIR (the NIST X-ray optics CALIBration Interferometer).

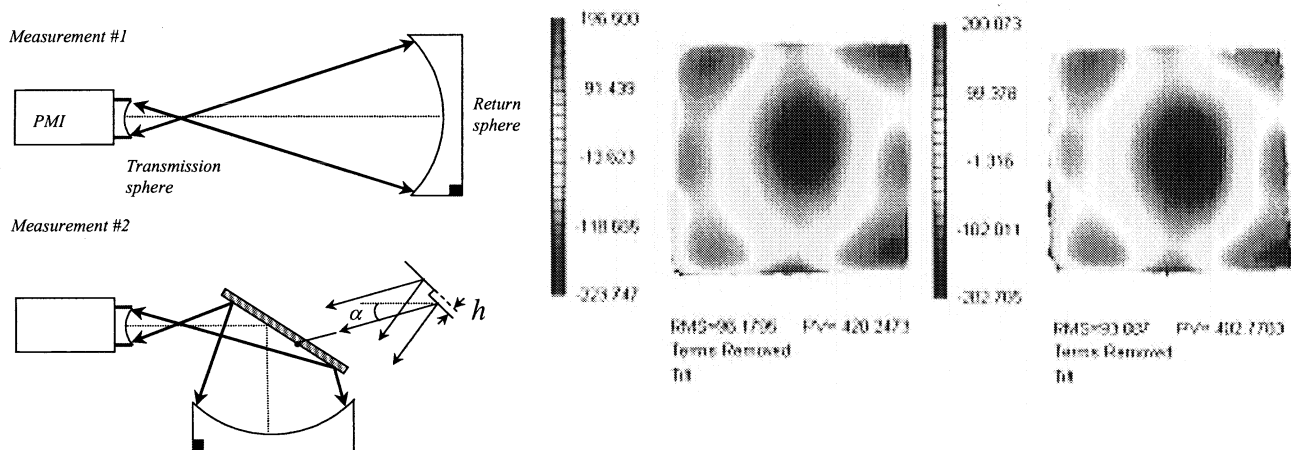


Figure 11 (Left) Schematic of the set-ups used in a Ritchey-Common test and (right) two independent measurements of the same photomask blank

8. CONCLUDING REMARKS

This paper has attempted to state the conditions to be met in order that a measurement of optical figure or wavefront may be reasonably claimed to be "traceable". For the majority of such measurements, it is straightforward to realize the unit length with an uncertainty sufficiently low to be ignored. The difficulty in deriving a defensible uncertainty statement is similar

when “self-calibration” is adopted rather than the conventional hierarchical calibration approach. Facilities and current projects at NIST designed to help industry achieve traceable measurements of figure or wavefront have been surveyed.

9. ACKNOWLEDGEMENTS

The authors are grateful to W. T. Estler for his reading of the manuscript and helpful comments.

10. REFERENCES

- 1 International Organization for Standardization (ISO) International Standard 14253-1, Geometrical product
2 Specification (GPS) – Part 1: Decision rules for proving conformance or non-conformance with specification
3 International Organization for Standardization (ISO), Guide to the Expression of Uncertainty in Measurement ,
4 Geneva, 1995
5 International Organization for Standardization, International Vocabulary of Basic and General Terms in Metrology,
6 Geneva, 1993
7 <http://www.nist.gov/traceability>
8 Evans C. J. , Hocken R. J., and Estler W. T. "Self-calibration: reversal, redundancy, error separation, and 'absolute
9 testing'" CIRP Annals, Vol 45/2 (1996) pp617-34
10 Stone J. Personal communication, 2000
11 Estler, W. T., 1985, “High accuracy displacement interferometry in air”, Appl Opt, Vol 24 / 6
12 Taylor B. N. and Kuyatt C. E. “Guide for Evaluating and Expressing the Uncertainty of NIST Measurement
13 Results” NIST Technical Note 1297, 1994
14 Estler, W. T. “Measurement as Inference: Fundamental Ideas” CIRP Annals, Vol 48/2 (1999)
15 Evans C. J and Kestner R. N. "Test optics error removal" Applied Optics Vol 35 (1996) pp1015-21
16 Specific commercial equipment is identified to fully describe the experimental procedures. Such identification does
17 not imply any endorsement of the product by the National Institute of Standards and Technology, nor that the
18 product is necessarily the best for the purpose.
19 Tropel Corp, Fairport, NY¹³
20 Specific commercial equipment is identified to fully describe the experimental procedures. Such identification does
21 not imply any endorsement of the product by the National Institute of Standards and Technology, nor that the
22 product is necessarily the best for the purpose.
23 Tropel Corp, Fairport, NY¹³
24 International Organization for Standardization (ISO) International Standard 1, Standard reference temperature for
25 industrial length measurements
26 Schmitz T. S., Davies A., and Evans C. J. “Uncertainties in interferometric measurements of radius of curvature”
27 Proc SPIE, Vol 4451, in press,
28 Bryan J. B. “Thermal Effects” CIR Annals Vol 39/2 (1990) p. 645
29 American National Standards Committee B89, ANSI B.89.6.2 “Temperature and Humidity Environment for
30 Dimensional Measurement” 1972, reaffirmed 1988
31 At the time of writing, the status of the document is unclear
32 Parks R. E., Shao L-Z., and Evans C. J. “Pixel-based absolute topography test for three flats” Applied Optics, Vol
33 37 (1998) pp5951-6
34 Estler W. T., Evans C. J. and Shao L-Z. "Uncertainty Estimation for Multi-Position Form Error Metrology"
35 Precision Engineering, Vol 21 (1997) pp72-82
36 Davies A. and Evans C. J. “Traceable measurement of a 300 mm optical flat: a complete evaluation of the
37 measurement uncertainty for a self-calibration test” Proc SPIE, Vol 4451, in press
38 Davies A. and Levenson M., Applied Optics, in press
39 Evans C. J., Parks R. E, Shao L-Z., and Davies A. “Interferometric metrology of photomask blanks: Approaches
40 using 633 nm wavelength illumination”, NISTIR 6701, December 2000
41 <http://www.phase-shift.com/optiflat.shtml>
42 Schwider J. “White light interferometer”, Applied Optics, 36(7) 1433-7 (1997)
43 de Groot P, Deck L., and Colonna de Lega C. “Adjustable coherence depth in a geometrically desensitized
44 interferometer”, SPIE 1998 Annual Meeting Paper # 3479-02
45 Ai C. “Multimode laser Fizeau interferometer for measuring the surface of a thin transparent plate” Applied Optics,
46 36(31) 8135-8 (1997)